
PHYLOGRAMS BETTER FIT NEUTRALLY EVOLVING TRAITS THAN CHRONOGRAMS

Thibault Latrille¹, Théo Gaboriau¹, Nicolas Salamin¹

¹Department of Computational Biology, University of Lausanne, Quartier Sorge, 1015 Lausanne, Switzerland

thibault.latrille@ens-lyon.org

March 27, 2026

Abstract

1 At the species level, the evolution of traits is driven by a combination of selective and
2 neutral forces. To disentangle these processes, different scenarios of evolution are modelled
3 and compared. For quantitative traits under selection, the species is usually considered to
4 track a trait optimum, and such an optimum can change along the branches of the species
5 tree. On the other hand, neutral evolution is modelled with a trait changing randomly
6 around the ancestral trait value along the different branches of the species tree. Regardless
7 of the intricacy of modelling trait changes, the species tree is assumed to be known and
8 obtained independently of the trait data analysed. Branch lengths are usually assumed to
9 be in units proportional to time, and the tree is represented by a chronogram. The rationale
10 is that time correlates with trait changes because of its direct connection with the number
11 of generations that have occurred. However, since the generation time of species can also
12 vary along the phylogenetic tree, we argue that their use introduces biases. In contrast, if
13 the phylogenetic tree is represented by a phylogram with branch lengths in units of sequence
14 divergence, this will account for the effect of changing generation time. In this study, we show
15 using simulations that, for a trait evolving neutrally, the fit of a random evolution model
16 has more support on a phylogram than on a chronogram. However, comparing models and
17 testing different scenarios of selection using a phylogram leads to incorrect predictions. Given
18 these results, we argue that we should use phylograms instead of chronograms when claiming
19 that a trait is evolving under drift. Nevertheless, we support the generally accepted use of
20 chronograms to model selection acting on a quantitative trait.

21 **Keywords** Comparative studies · Morphological evolution · Genetic drift · Macroevolution · Chronogram ·
22 Phylogram

23 Teaser text

24 Many species, are characterised by trait differences between each other. For example, the brain size of
25 different primate and human lineages varies. The question we ask is: Does the time that passed explain the
26 differences in their traits? Or are genetic differences between species better at explaining the differences? The
27 standard in evolutionary biology is to use time to explain differences in traits. However, if the trait is not
28 under natural selection and instead is changing due to the accumulation of neutral substitutions (because of
29 genetic drift), the genetic differences between species should better explain the differences in traits than the
30 time since divergence. As a result, we argue that using both genetic differences and species divergence time
31 simultaneously provides a better understanding of how traits evolve across species.

32 Introduction

33 By measuring changes in a phenotypic trait along a lineage, it is possible to infer the type of selection
34 acting on it or whether this change is only due to random genetic drift. At a larger scale, from the observed
35 variations of traits across species, regimes of evolution are typically assessed using phylogenetic comparative
36 methods, where traits are modelled as evolving along the branches of the species tree (Felsenstein, 1985,
37 1988; Harmon, 2018). For example, to model neutral evolution, the mean trait value is said to follow a
38 Brownian motion (BM), branching and evolving independently after each speciation event (Felsenstein,
39 1985; Hansen and Martins, 1996; Lynch and Hill, 1986). In other words, for each branch of the tree, the
40 value at the descendant node is normally distributed around the ancestral value, with a variance proportional
41 to the branch length. In this framework, reconstructing trait variation along the whole phylogeny as a BM
42 process can thus constitute a null model of neutral trait evolution, although as we discuss later, BM can also
43 approximate non-neutral evolutionary processes.

44 Alternatively to a simple BM, adding a trend parameter in the BM is interpreted as a signature of direc-
45 tional selection at the phylogenetic scale, reflecting a consistent bias in trait evolution across lineages (Sil-
46 vestro et al., 2019). However, such trends can be difficult to distinguish from BM in analyses using only
47 extant taxa without fossil calibration (Felsenstein, 1988). More complex models to detect selection have
48 been proposed, notably the Ornstein-Uhlenbeck (OU) processes, where trait variation is constrained around
49 an optimum value, which is often interpreted as a signature of stabilizing selection (Beaulieu et al., 2012;
50 Butler and King, 2004; Hansen, 1997). Methodologically, this alternative model of evolution raises issues
51 since an OU process might be statistically preferred over BM due to sampling artifacts (Cooper et al., 2016;
52 Price et al., 2022; Silvestro et al., 2015). Adding biological realism, the OU process can be relaxed to allow
53 for multiple optima along the phylogenetic tree, which is interpreted as a few abrupt changes in the envi-
54 ronment along the phylogeny (Grabowski et al., 2023; Ingram and Mahler, 2013; Khabbazian et al., 2016;
55 Mitov et al., 2020; Uyeda and Harmon, 2014). Finally, the optimum can also be allowed to change contin-
56 uously along the tree, which results in the trait itself reflecting the movement of the optimum along the
57 lineages due to the constant adaptive evolution of the trait toward the optimum (Hansen, 2024; Hansen and
58 Martins, 1996). One special case of a continuously changing optimum is again the BM, where changes in the
59 optimum are a consequence of the randomly changing environment (Hansen et al., 2008), named fluctuating
60 selection (Holstad et al., 2024) or also diversifying selection due to the diversity of generated phenotypes at
61 the clade level (Latrille et al., 2024). This modelling raises an issue in disentangling selection from neutral
62 evolution: the fact that BM is the best-supported model in a set does not necessarily imply that a trait is
63 evolving neutrally. In other words, Brownian evolution can also result from non-neutral evolutionary pro-
64 cesses, such as stabilizing selection on an optimum that moves as a BM in time, or such as fluctuating natural

65 selection. More generally, due to the central limit theorem, the additive effects of many different neutral and
 66 non-neutral random factors might result in evolution that appears Brownian.

67 To disentangle neutral evolution from different regimes of selection, another approach is to contrast the
 68 observed rate of evolution to the neutral expectation (Lande, 1980). The neutral expectation can be obtained
 69 if the underlying genetic architecture of the trait is known and the trait is encoded by many loci of additive
 70 effects (Barton et al., 2017; Sella and Barton, 2019). Additionally, we can also derive the expected changes
 71 in mean trait value along a lineage given the trait variance at the population scale (Felsenstein, 1988; Lynch,
 72 1990; Turelli, 1984, 1988). When generalized to many species at the phylogenetic scale, contrasting between
 73 and within-species variations allows us to disentangle neutral evolution from selection tracking a moving
 74 optimum. Specifically, Latrille et al. (2024) showed that the ratio of between-species to within-species trait
 75 variation should scale linearly with nucleotide divergence for a neutral trait, providing a neutrality test that
 76 requires both types of variation data. However, such within-species variation data are not always available,
 77 motivating the current study, which focuses solely on between-species variation and tree branch length
 78 units. More generally, comparing the rate of evolution at different timescales allows inferring the regime of
 79 evolution (Hansen, 2024; Holstad et al., 2024). However, trait variation at different timescales is not always
 80 available, and the genetic architecture of the trait is often unknown. Instead, to disentangle neutral evolution
 81 from selection tracking a moving optimum in the context of phylogenetic comparative methods, we hereby
 82 focus on the underlying tree and the unit of its branch lengths (Fig. 1A).

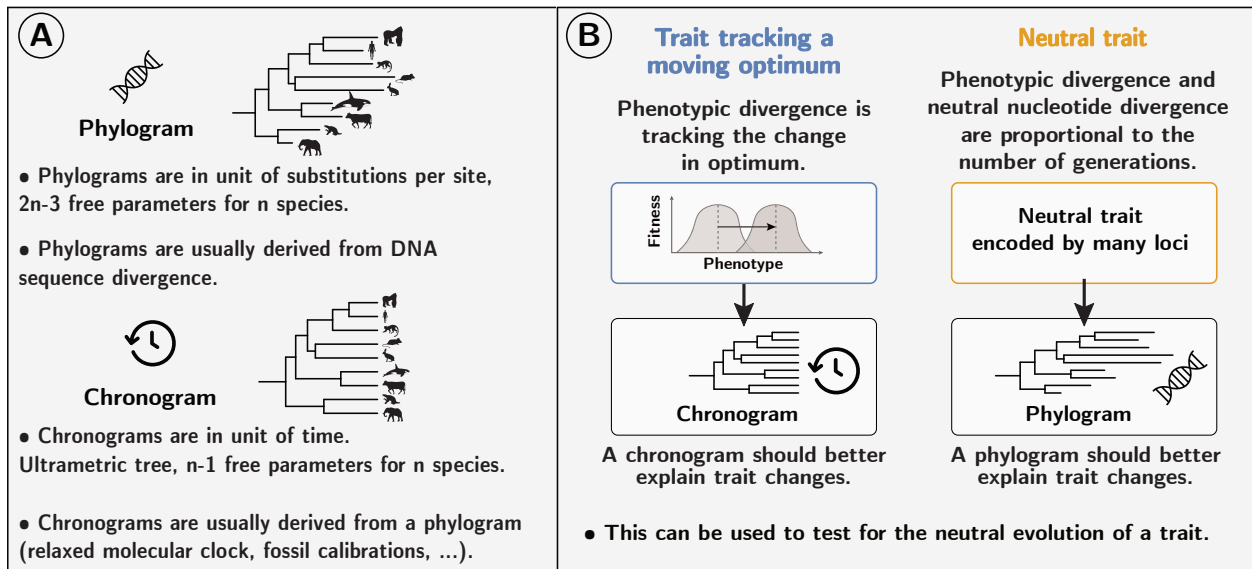


Figure 1: Panel A: Across many species, the evolution of continuous traits can be modelled as a stochastic process evolving along the branches of a phylogenetic tree. The branches of such a phylogenetic tree can be measured in either time (chronogram) or number of substitutions (phylogram). Panel B: Theoretically, changes of a trait under a moving optimum should be better predicted by a chronogram than by a phylogram, since the optimum is expected to change with time rather than with the number of generations. Conversely, changes of a neutral trait should be better predicted by a phylogram than by a chronogram, since neutral trait changes are proportional to the number of generations (and thus nucleotide divergence), not time. Comparing the fit of a BM process on both trees can help disentangle neutral evolution from selection tracking a moving optimum. Alt text: Schematic representation of the rationale to use a phylogram or a chronogram to model trait evolution.

83 Typically, the tree is assumed to be known and obtained independently, and the *de facto* standard in
 84 phylogenetic comparative methods is to use a chronogram, where the branch lengths are proportional to
 85 time (Felsenstein, 1985; Harmon, 2018). Theoretically, for a neutrally evolving trait, trait changes depend
 86 directly on the number of generations (Hansen and Martins, 1996), which is proportional to time only if
 87 the average time between two consecutive generations, called generation time, is constant and equal for all
 88 species. Since generation time depends on the time for an individual to reach sexual maturity, it can vary
 89 considerably between species, even within a single clade. For example, in mammals, generation time ranges
 90 from less than a year in mice to over 20 years in elephants (De Magalhães and Costa, 2009), representing
 91 variation that could substantially impact inferences of neutral trait evolution. As a result, variations of
 92 generation time between species suggest that modelling neutral evolution as BM on a chronogram induces
 93 biases (Litsios and Salamin, 2012).

94 Alternatively, on a phylogram, branch lengths represent another quantity than time, which can be used as
 95 the backbone to model trait evolution and can potentially absorb changes in generation time. For example,
 96 it is known that using phylograms in units of morphological distance can be used to improve ancestral trait
 97 reconstruction for a discrete character (Wilson et al., 2022). From a genomic perspective, phylograms can
 98 also be in units of nucleotide divergence, that is, depicting the number of nucleotide substitutions occurring
 99 along a branch. Because the number of neutral nucleotide substitutions accumulating along a branch is
 100 proportional to the number of generations (Kimura, 1968, 1983), nucleotide divergence would in this case
 101 absorb the effect of changing generation time (i.e. longer branches for lineages with shorter generation time).
 102 Such a phylogram, if obtained from neutrally evolving genomic loci would be more appropriate to model a
 103 trait evolving neutrally (Latrille et al., 2024). More precisely, under the assumption of a constant genetic
 104 architecture, the covariance in mean trait value between a pair of species increases linearly with the number
 105 of shared generations, and thus with shared nucleotide divergence for neutral sequences (see Supplementary
 106 Material section S1 for the theoretical derivation). Additionally, the rationale to use nucleotide divergence
 107 to absorb changes in generation time is also valid for changes in mutation rate (per loci and per generation)
 108 under the assumption of a constant genetic architecture of the trait and that changes in mutation rate impact
 109 the whole genome (Latrille et al., 2024). Empirically, such changes in mutation rate along a phylogenetic
 110 tree are also observed, although to a lesser extent than changes in generation time (Bergeron et al., 2023).

111 Under the alternative scenario involving selection, shorter generation time and higher mutation rate can
 112 also allow for the species to track the changing optimum faster and not lag behind (Hansen et al., 2008;
 113 Lande, 1976). However, the timescale for this adaptive lag (typically hundreds to thousands of generations)
 114 is negligible compared to the timescale on which the optimum changes at the level of clades (millions of
 115 years) in a first approximation (Hansen, 2024). While this lag timescale is difficult to measure empirically,
 116 theoretical considerations suggest it should be much shorter than the macroevolutionary timescale. Thus, at
 117 the phylogenetic scale, since shifts in the optimum fitness peak are extrinsic to the species and are dependent
 118 on the environment which varies with time, using a chronogram would be more accurate to model mean trait
 119 changes. As a result, for a trait under selection, mean trait changes should be better explained by the time
 120 rather than the number of substitutions that occurred along a branch (Fig. 1B).

121 In this study, we test this hypothesis, namely whether using a phylogram (in units of nucleotide divergence
 122 for neutral loci) instead of a chronogram (in units proportional to time) can allow to assess the evolutionary
 123 regime of a trait, by evaluating the fit of BM on both trees. More precisely, we seek to test whether the changes
 124 of a neutral trait are better predicted by a phylogram. Conversely, we also seek to test whether changes of
 125 a trait under a moving optimum are better predicted by a chronogram. Using genomic information, we seek

126 to provide additional approaches to model trait evolution, particularly to disentangle neutral evolution from
 127 selection tracking a moving optimum.

128 **Methods**

129 To assess whether a phylogram is better suited to model neutral evolution, we first performed simulations
 130 of a trait evolving along a phylogenetic tree under different regimes of selection (neutral, moving optimum,
 131 multiple optima). Second, we fitted a single-rate Brownian motion (BM) to the simulated data, and we
 132 compared the fit of the BM on a phylogram versus a chronogram. Third, based on the single-rate BM, we
 133 derived a model to estimate the support of a phylogram over a chronogram that we apply to the simulated
 134 dataset. Fourth, we fitted several models of trait evolution to the simulated datasets: a multi-rate BM, an
 135 Ornstein-Uhlenbeck (OU) process, and a relaxed OU with multiple optima, tested on a phylogram versus a
 136 chronogram. Finally, we gathered an empirical dataset of body and brain masses from mammals, including
 137 both a chronogram and a phylogram (in units of nucleotide divergence from neutral loci), on which we tested
 138 the support of a phylogram for the single-rate BM. To assess which tree type (phylogram versus chronogram)
 139 better supports neutral evolution, we evaluate both the statistical fit of the BM and the accuracy of ancestral
 140 trait reconstruction under each tree.

141 **Simulations along a phylogenetic tree**

142 We performed simulations under different selective regimes (neutral, moving optimum, multiple optima).
 143 Simulations were individual-based and followed a Wright-Fisher model with mutation, selection and drift for
 144 a diploid population including speciation along a predefined ultrametric phylogenetic tree. We used the same
 145 simulation framework as in [Latrille et al. \(2024\)](#), with parameters detailed in the Supplementary Material
 146 (section S2). The parameters of simulations were chosen to mimic an empirical dataset of mammals. In
 147 summary, the trait was encoded by L independent loci (Fig. S1), with each locus contributing additively, and
 148 mutations were drawn from a Poisson distribution at each generation. Parents were selected for reproduction
 149 according to their phenotypic value, with a probability proportional to their fitness. Flattening the fitness
 150 landscape resulted in neutral evolution, which meant that each individual had the same probability of being
 151 sampled at each generation regardless of its trait value. Alternatively, for a trait under selection around a
 152 moving optimum, we modelled stabilizing selection acting on the trait, with the optimum value changing as
 153 a geometric Brownian motion (BM) along the phylogenetic tree ([Hansen, 1997](#); [Hansen and Martins, 1996](#)).
 154 Finally, for a trait under selection around multiple optima ([Uyeda and Harmon, 2014](#)), we draw a Bernoulli
 155 variable to test whether there is a switch of optimum along a branch; if a switch occurs, the sliding of the
 156 optimum is drawn from a reflected exponential distribution (symmetric positive and negative values).

157 At each internal node of the tree (i.e. speciation event), the population is split into two daughter pop-
 158 ulations running independently on each of the two branches, and the process is repeated until the tips of
 159 the tree are reached. As a control, we performed simulations with constant mutation rates, generation times
 160 and effective population sizes (N_e). Alternatively, we performed simulations with fluctuating mutation rates,
 161 generation times and N_e , where we used BM to model the long-term changes along the phylogenetic tree,
 162 and we overlaid short-term changes in N_e (see Supplementary Material section S2).

163 The phylogram is obtained from the same simulation setting on a set of 30,000 independent neutral loci,
 164 and the nucleotide divergence is computed as the number of substitutions along each branch. The chronogram
 165 is the generating ultrametric time tree used in the simulation. For the empirical datasets, the chronogram is

166 derived from the phylogram by fitting a relaxed molecular clock model (correlated rate model with penalized
167 likelihood, default value) to the phylogram with the *R* package *ape* (Paradis et al., 2004).

168 **Brownian motion (BM)**

169 On the simulated dataset, we fitted a single-rate BM using either a phylogram or a chronogram as the
170 underlying tree. We used *RevBayes* (Höhna et al., 2016) to fit a Brownian motion (BM) on continuous traits
171 evolving along the branches of a phylogenetic tree (Felsenstein, 1985, 1988). The data consist of the mean
172 trait value for each extant species, and the tree topology is fixed. Along each branch, the value of the trait
173 is drawn from a normal distribution with mean equal to the parent node value and variance equal to the
174 branch length (Felsenstein, 1985). Formally, the BM process is described by the equation:

$$dP_t = \sigma \cdot dW_t, \quad (1)$$

175 where P_t is the trait value at time t , σ is the rate of the BM, and dW_t is a Wiener process (i.e. a standard
176 Brownian motion). We used a log-uniform prior for σ . Using Markov chain Monte Carlo (MCMC), we
177 reconstructed the ancestral trait value at each node of the tree as the posterior mean estimate (burn-in
178 of 1000 gen., running of 10,000 gen., 2 chains), and we compared the accuracy of the reconstruction using
179 either a phylogram or a chronogram as the underlying tree. Both trees are scaled such that the sum of all
180 the branch lengths is equal to one in each case. Importantly, the data and the tree topology are the same
181 in both analyses; only the branch lengths are different. In this simulation setting, for traits simulated under
182 neutral evolution, we expect more accurate trait reconstruction on a phylogram, and conversely, for traits
183 under selection (moving optimum), more accurate trait reconstruction on a chronogram.

184 **BM with a switch**

185 To test the support of a phylogram over a chronogram, we implemented a model based on a single-rate BM.
186 The model was implemented in *RevBayes* and contains a switch variable, denoted as π that allows the model
187 to switch the branch lengths in units of time to units of substitutions (Fig. 2A). Formally, π is a Bernoulli
188 random variable ($\pi \in \{0, 1\}$) with a prior probability of 0.5. If π is 0, the branch lengths are those of the
189 chronogram, and if π is 1, the branch lengths are those of the phylogram. The tree topology is fixed, meaning
190 both trees have the same branching structure, but because branch lengths are different and not necessarily
191 on the same scale, both trees are re-scaled by dividing branch lengths by the total tree length. As in the
192 previous section, BM is fitted to the data by modelling trait changes as normal distributions (*dnNormal*
193 in *RevBayes*) running along the branches of the tree, with variance proportional to the branch length and
194 the squared value of the Brownian rate parameter (σ , log-uniform prior). Alternatively for large trees or for
195 faster computation, the likelihood can also be estimated by the REML method (*dnPhyloBrownianREML* in
196 *RevBayes*). Altogether, the input data is the mean trait value for extant species and both the chronogram
197 and phylogram with the same tree topology. The posterior mean of π (burn-in of 1,000 gen., running of
198 10,000 gen., 2 chains) indicates support for the phylogram; we consider the phylogram to be favoured when
199 $\pi > 0.5$. We expect $\pi = 1$ for a trait under neutral evolution, and $\pi = 0$ for a trait under selection (moving
200 optimum).

201 From a maximum likelihood perspective, the support of a phylogram over a chronogram can also be
202 assessed by model selection, by comparing the maximum likelihood of the data given each tree, and computing
203 the Akaike Information Criterion (AIC) weights of each model (see Supplementary Material section S5).

204 Alternative models of evolution

205 In addition to a single-rate BM, we also fitted BM with multiple rate parameters (Eastman et al., 2011),
 206 using either a phylogram or a chronogram as the underlying tree to the simulated dataset. The likelihood of
 207 the data is estimated by the REML method (*dnPhyloBrownianREML* in *RevBayes*), and the number of rate
 208 shifts is estimated by reversible-jump MCMC (*dnReversibleJumpMixture* in *RevBayes*). For each branch,
 209 we draw a rate-multiplier either equal to 1 (no rate shift), or drawn from a log-normal distribution with a
 210 median of 1, and a standard deviation such that rate shifts range over about one order of magnitude. We
 211 set our prior to the expected number of rate shifts of 1 across the whole tree. The number of rate shifts as
 212 well as the variance of rate parameters are estimated as the posterior mean (burn-in of 1,000 gen., running
 213 of 50,000 gen., 2 chains).

214 Also, we compared the fit of an Ornstein-Uhlenbeck (OU) process (eq. 2) to BM (Butler and King, 2004;
 215 Hansen, 1997), using either a phylogram or a chronogram as the underlying tree. The OU process is described
 216 by the equation:

$$dP_t = -\alpha (P_t - \theta) dt + \sigma \cdot dW_t, \quad (2)$$

217 where the parameter α in eq. 2 is the strength of the pull towards the optimum, θ is the optimum value
 218 and the other parameters are defined as in eq 1. The likelihood of the data is estimated by the REML
 219 method (*dnPhyloOrnsteinUhlenbeckREML* in *RevBayes*), and because the OU process has more parameters
 220 than the BM, we used a reversible-jump MCMC switch between the two models (0 for BM and 1 for OU,
 221 *dnReversibleJumpMixture* in *RevBayes*). The prior for θ is uniform between the minimum and maximum
 222 trait value for extant species. The prior for α is a reversible-jump mixture distribution: a value of 0 or drawn
 223 from an exponential distribution with mean equal to half the root age divided by $\ln(2)$, meaning that we
 224 expect a phylogenetic half-life of half the crown age. Thus, when $\alpha = 0$ the OU process (eq. 2) is equivalent
 225 to BM (eq. 1). The half-life, $t_{1/2}$, is defined as $\ln(2)/\alpha$ is also estimated as the posterior mean estimate of
 226 finite values (burn-in of 1,000 gen., running of 5,000 gen., 2 chains), representing the time needed for the
 227 expected trait value to move half-way toward the optimum (Grabowski et al., 2023; Hansen, 1997),

228 Finally, we fitted a relaxed OU with multiple optima (Uyeda and Harmon, 2014), using either a phylogram
 229 or a chronogram as the underlying tree. The likelihood of the data given the tree is estimated by the REML
 230 method (*dnPhyloOrnsteinUhlenbeckREML* in *RevBayes*), and the number of optimums is also estimated by
 231 the reversible-jump MCMC method (*dnReversibleJumpMixture* in *RevBayes*) as the posterior mean estimate
 232 (burn-in of 1,000 gen., running of 5,000 gen., 2 chains). For each branch, we draw a shift in optimum either
 233 equal to 0 (no shift), or drawn from a uniform distribution centred on 0 with breadth spanning the whole
 234 range of observed trait value. We set our prior to the expected number of optimum shifts of 1 across the
 235 whole tree.

236 Empirical dataset

237 We analysed a dataset of body and brain masses from mammals. The log-transformed values of body and
 238 brain masses were taken from Tsuboi et al. (2018). We removed individuals not marked as adults and split
 239 the data into males and females due to sexual dimorphism in body and brain masses. We also extracted
 240 brain and body masses from the *COMBINE* dataset (Soria et al., 2021). The mammalian genomic data are
 241 gathered from the Zoonomia project (Genereux et al., 2020). More specifically, the phylogram in units of
 242 nucleotide divergence is estimated on a set of neutral markers in Foley et al. (2023). The chronogram is
 243 derived from the phylogram by fitting a relaxed molecular clock model (correlated rate model with penalized
 244 likelihood, default value) to the phylogram with the *R* package *ape* (Paradis et al., 2004).

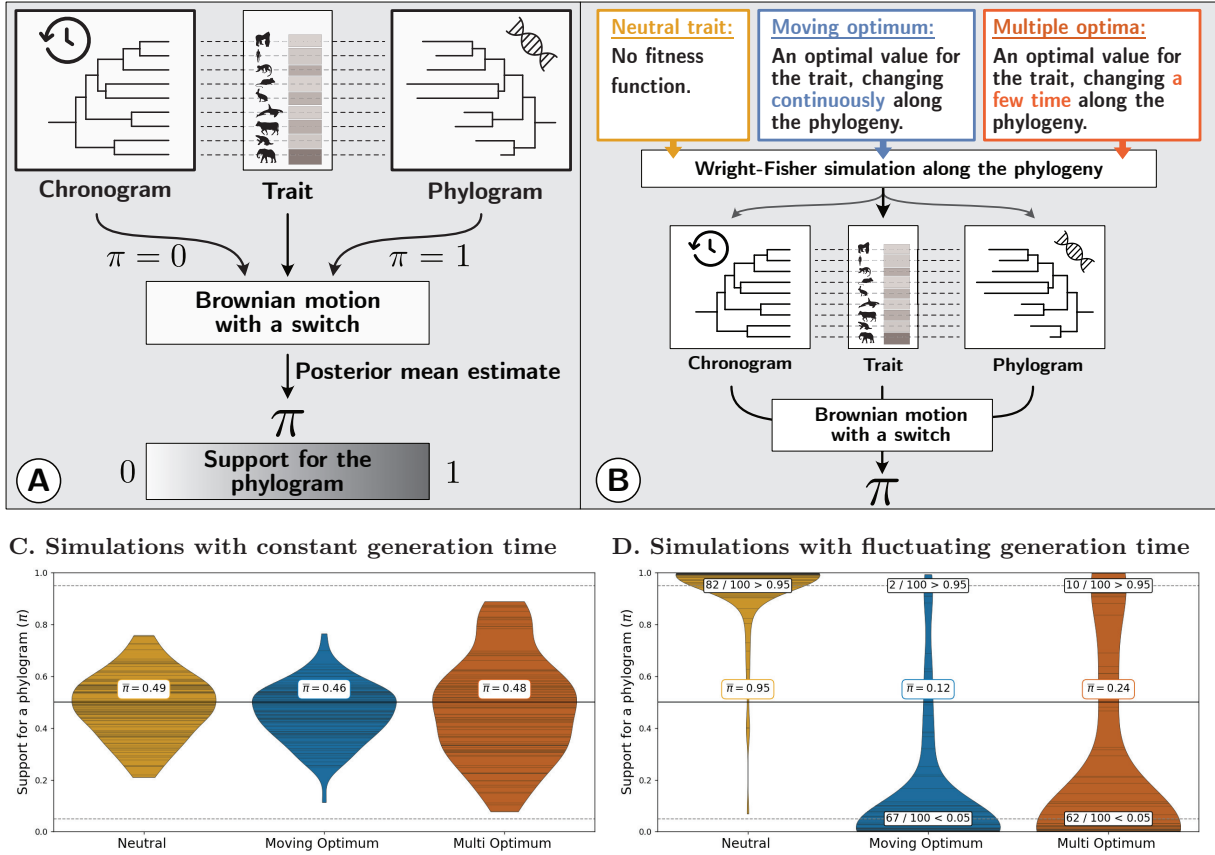


Figure 2: Testing the support for a phylogram over a chronogram Panel A: Brownian motion (BM) is used to model trait changes along a phylogeny, given a mean trait value for extant species. The model contains a switch variable, denoted π , that switches the branch lengths in units of time ($\pi = 0$, chronogram) to units of nucleotide divergence for neutral sites ($\pi = 1$, phylogram). The posterior mean estimate of π indicates whether BM supports the phylogram better than the chronogram ($0 \leq \pi \leq 1$). Panel B: Wright-Fisher simulations of trait evolution along a phylogeny. At each node of the tree a speciation event creates two descendant species evolving independently. Neutral evolution is modelled as a constant fitness regardless of the phenotype of individuals (yellow). Selection is modelled by stabilizing selection around an optimum value, which is changing along the phylogenetic tree: as a moving optimum (blue) or as multiple optima (red). The output of the simulation is: 1) the mean trait value for each extant species, 2) the phylogram as obtained from independent neutral markers and 3) the chronogram derived from the phylogram assuming a relaxed molecular clock. The posterior mean estimate of π is inferred from the output of the simulation. Panels C & D: Violin plot of the posterior mean of π across 100 replicates for the different simulated regimes of evolution with mean π values at the center ($\bar{\pi}$). Horizontal lines inside the violins are the estimated π of each replicate simulation. Results of simulations with constant generation time (Panel C) and with fluctuating generation time, mutation rate and effective population size (Panel D). Alt text: Results of simulations testing the support for a phylogram over a chronogram under different regimes of evolution.

245 Results

246 Support for a phylogram over a chronogram

247 We tested the hypothesis that a phylogram is better suited to model neutral evolution than a chronogram.
 248 We simulated traits evolving on a phylogenetic tree under different regimes of selection: 1) neutrally evolving,
 249 2) under a moving optimum, and 3) under multiple optima (see Methods). We first assessed the accuracy
 250 of ancestral trait reconstruction on a phylogram versus a chronogram, under the assumption that changes
 251 follow BM. For a neutral trait, ancestral trait reconstruction was more accurate on a phylogram (Fig. S2A,
 252 $r^2 = 0.95$) than on a chronogram (Fig. S2B, $r^2 = 0.83$; Fisher’s z -test, $p_{\text{value}} = 9.0 \times 10^{-11}$). In contrast, for
 253 a trait evolving under a moving optimum, ancestral trait reconstruction was less accurate on a phylogram
 254 (Fig. S2C, $r^2 = 0.79$) than on a chronogram (Fig. S2D, $r^2 = 0.96$; Fisher’s z -test, $p_{\text{value}} = 0$).

255 We then tested for the BM support of phylogram over a chronogram, and we developed a statistic
 256 denoted as π (Fig. 2A), which ranges from 0 (full support for the chronogram) to 1 (full support for the
 257 phylogram). For simulations with a constant generation time, the support is similar for both a phylogram and
 258 a chronogram regardless of the regime of evolution (Fig. 2B-C), which is expected since the branch lengths
 259 are equivalent in both trees. Next, we simulated changing generation time, mutation rate (per generation)
 260 and effective population size (N_e) along the phylogenetic tree, mimicking a mammalian range of changes. In
 261 this case, for a simulated neutral trait, the BM was better fitted on a phylogram than on a chronogram, with
 262 an average support for phylogram of $\bar{\pi} = 0.95$ across 100 replicate simulations, and 82 of the 100 replicates
 263 above the 0.95 threshold (Fig. 2D, yellow). Conversely, for a simulated trait under selection, the fit of BM on
 264 a chronogram was better than on a phylogram with an average support for phylogram of $\bar{\pi} = 0.12$ for multiple
 265 optima (67 out of 100 replicates below the 0.05 threshold, Fig. 2D, blue) and $\bar{\pi} = 0.24$ for a moving optimum
 266 (62 of the 100 below the 0.05 threshold, Fig. 2D, red). Finally, from a statistical perspective, the equivalent
 267 of π using the maximum likelihood approach (AIC weights, see Supplementary Material section S5) is highly
 268 correlated with our Bayesian estimate ($r^2 = 0.99$, Fig. S3).

269 On the empirical mammalian dataset from Tsuboi et al. (2018), for body mass the support for the
 270 phylogram is $\pi = 0.0$, when sex is not taken into account. When splitting the dataset into males and
 271 females, the support for the phylogram is $\pi_{\text{♀}} = 0.85$ and $\pi_{\text{♂}} = 0.70$. For brain mass, the support for the
 272 phylogram is $\pi = 0.0035$ on the mixed dataset, with $\pi_{\text{♀}} = 0.56$ and $\pi_{\text{♂}} = 0.51$. On the *COMBINE* dataset,
 273 which does not distinguish between males and females, the support for the phylogram is $\pi = 0.0$ for body
 274 mass and $\pi = 0.0015$ for brain mass (Table S1). We also computed π using an approximate likelihood
 275 computation (REML), a method that allow for faster computation and scale better for larger trees, and
 276 found similar results (Table S1).

277 Fitting alternative models of evolution

278 Besides testing the fit of BM with a single-rate, we also fitted a multi-rate BM (see Methods) to simulated
 279 datasets with changing generation time, mutation rate and effective population size (N_e). When fitting a
 280 multi-rate BM, the estimated variance of rate parameters (v) was lower on a phylogram than on a chronogram
 281 for a trait evolving neutrally (Fig. 3A, yellow violins, Wilcoxon paired test with $p_{\text{value}} = 4.5 \times 10^{-13}$), and the
 282 number of rate shifts (n) was reflecting the prior on the phylogram while not on the chronogram, showing a
 283 bias (Fig. 3B, yellow violins). Conversely, for a trait under a moving optimum, v was higher on a phylogram
 284 than on a chronogram (Fig. 3A, blue violins, Wilcoxon paired test with $p_{\text{value}} = 1.3 \times 10^{-14}$), and n was
 285 reflecting the prior on the chronogram while not on the phylogram, showing a bias (Fig. 3B, blue violins).

286 Altogether, fitting BM on a phylogram is more accurate for a trait evolving neutrally, but results in less
 287 accurate estimates for a trait under selection.

288 Moreover, we tested alternatives to the BM with OU models: with a single optimum and with multiple
 289 optima (see Methods). Following recommendations by [Grabowski et al. \(2023\)](#), we report the phylogenetic
 290 half-life ($t_{1/2} = \ln(2)/\alpha$), which represents the time for a trait to evolve halfway toward a new optimum.
 291 The higher the half-life, or in other words, the smaller the α , the more the OU process becomes effectively
 292 indistinguishable from BM. For a trait evolving neutrally, the estimated half-life was longer on a phylogram
 293 than on a chronogram (Fig. 3C, yellow violins, Wilcoxon paired test with $p_{\text{value}} = 4.9 \times 10^{-5}$), confirming
 294 BM-like dynamics on phylograms as expected for neutral evolution. Conversely, for a trait under a moving
 295 optimum, the half-life was shorter on a chronogram than on a phylogram (Fig. 3C, blue violins, Wilcoxon
 296 paired test with $p_{\text{value}} = 1.5 \times 10^{-12}$), indicating faster adaptation on the appropriate tree. When fitting a
 297 multi-OU process on a trait evolving neutrally, the number of optimum shifts (m) was reflecting the prior on
 298 the phylogram, but not on the chronogram (Fig. 3D, yellow violins). Conversely, for a trait under a moving
 299 optimum, (m) was reflecting the prior on the chronogram but not on the phylogram (Fig. 3D, blue violins).

300 Discussion

301 In phylogenetic comparative methods, the evolution of continuous traits is typically modelled as a stochastic
 302 process evolving along the branches of a phylogenetic tree. The null model of neutral trait evolution, genetic
 303 drift, is thought of as a Brownian motion (BM) running on the tree ([Felsenstein, 1988](#); [Lynch and Hill, 1986](#)),
 304 and deviations from this model are interpreted as selection acting on the trait ([Butler and King, 2004](#)). As
 305 a result, a trait on which the BM is favoured over alternative models are sometimes interpreted as a trait
 306 evolving neutrally ([Catalán et al., 2019](#); [Khaitovich et al., 2006](#)). However, the BM is not only the null
 307 model of neutral evolution, but can also model selection, with a trait tracking a moving optimum, where
 308 the optimum itself is following BM ([Hansen and Martins, 1996](#); [Latrille et al., 2024](#)). More fundamentally,
 309 the central limit theorem implies that trait evolution can appear Brownian whenever the trait is influenced
 310 by a large number of independent random factors acting additively ([Felsenstein, 1985](#)). These factors may
 311 include fluctuating genetic architecture, mutational pressures, changing population size, randomly changing
 312 environment, genetic drift, and natural selection. Some of these influences may vary in a manner more
 313 directly connected to generation time, while others may track real time, making it difficult to predict a priori
 314 which tree type should provide the better fit. Therefore, a good fit of BM alone cannot distinguish between
 315 neutral evolution and stabilizing selection on an optimum that moves as a BM, and the comparison between
 316 phylogram and chronogram provides a crucial additional diagnostic.

317 Distinguishing these scenarios is not trivial, but we here showed that the underlying backbone tree to
 318 model trait evolution can help disentangle neutral evolution from selection tracking a moving optimum. The
 319 standard in phylogenetic comparative methods is a chronogram, where the branch lengths are measured
 320 in time ([Felsenstein, 1985](#); [Harmon, 2018](#)), while phylograms, where the branch lengths are measured in
 321 number of substitutions instead, have been generally overlooked. For a simulated trait under selection we
 322 assessed that the BM has indeed a better fit on a chronogram than on a phylogram. However, we argue that
 323 to model a trait evolving neutrally, the backbone tree should not be a chronogram but instead a phylogram.
 324 Phylograms better represent the number of generations that occurred, and in turn should explain best the
 325 differences in traits between species ([Latrille et al., 2024](#)) In practice, we show that for simulations of a trait
 326 evolving neutrally, the fit of BM supports a phylogram rather than a chronogram. Additionally, for a neutral
 327 trait, both ancestral state reconstruction and estimation for the number of rate changes for a multi-rate BM

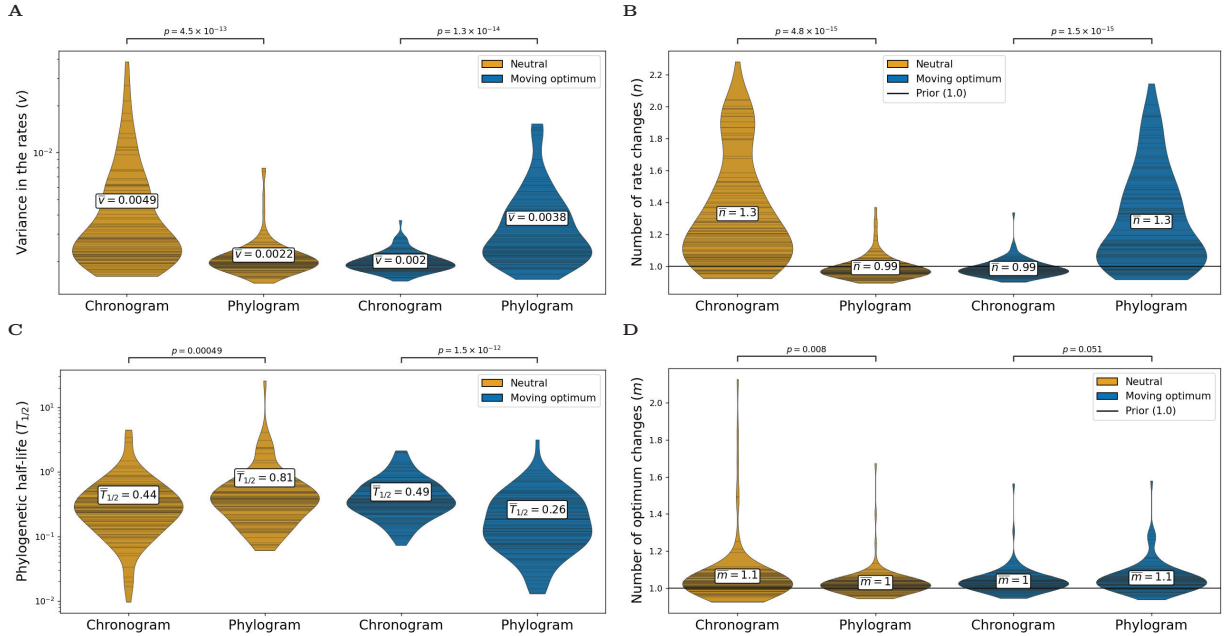


Figure 3: **Mis-classification of trait evolution on a phylogram.** Violin plot of posterior parameter estimates for different models of trait evolution and different simulated regimes of selection. Horizontal lines inside the violin show the results of each replicate simulation. Simulations of 100 replicates per regime: trait evolving under a neutral regime (yellow) and under a moving optimum (blue). Wilcoxon rank-test are performed between the paired estimates on the phylogram and the chronogram. Panel A & B: Fit of a relaxed Brownian motion (BM) with multiple rate parameters, using either a phylogram or a chronogram. Posterior estimate for the variance in rate parameters (Panel A) and number of rate changes (Panel B). Panel C: Estimated phylogenetic half-life ($t_{1/2} = \ln(2)/\alpha$) from an Ornstein-Uhlenbeck (OU) process, using either a phylogram or a chronogram. The half-life represents the time for a trait to evolve halfway toward the optimum; longer half-life indicates BM-like dynamics. Panel D: Fit of a relaxed OU with multiple optima, using either a phylogram or a chronogram. Posterior estimate for the number of optimum changes. Alt text: Violin plot of posterior parameter estimates for different models of trait evolution and different simulated regimes of selection.

328 was more accurate on a phylogram. Altogether, the combined use of a phylogram and a chronogram can
 329 help support the hypothesis of neutral evolution, or to rule it out.

330 We applied this method to different empirical datasets of body and brain masses in mammals, and we
 331 showed that the chronogram was favoured over the phylogram, ruling out the neutral model of evolution for
 332 these traits (Latrille et al., 2024). The mammalian dataset is particularly relevant, since changes in generation
 333 time are expected to occur along the phylogenetic tree, from 6 months for mice to 50 years for bowhead
 334 whales (De Magalhães and Costa, 2009; Nielsen et al., 2016). When analysing each sex separately, the dataset
 335 with annotated sex available is smaller (column Taxa in Table S1). Only 46 species have annotated sexes,
 336 compared to a range of 125–217 species when not specifying sex. On this dataset of 46 species, neither the
 337 phylogram nor the chronogram is favoured, with undecided support ($0.497 \leq \pi \leq 0.848$). This undecided
 338 result could reflect insufficient statistical power due to the small number of species, but other explanations
 339 are also possible: the true evolutionary process may not conform well to BM on either timescale, or it may

340 involve a combination of selective and neutral processes that does not clearly favour one tree type over the
 341 other.

342 More generally, our method is also relevant when changes in mutation rate (per generation) and effective
 343 population size (N_e) are expected. First, normalizing by nucleotide divergence also accounts theoretically
 344 for variations in effective population size (N_e) since the substitution rate of neutral mutations is equal to
 345 the mutation rate, such that N_e has no effect on the rate of neutral evolution (Kimura, 1968; Ohta, 1972).
 346 Moreover, if population structure were to impact the probability of fixation for neutral mutations (which
 347 would also impact a neutral trait), the phylogram would automatically absorb these changes. This argument
 348 was partially tested in our simulation by modelling changes in both N_e and generation time (although
 349 not modelling population structure *per se*), and the phylogram was favoured over the chronogram for a
 350 trait evolving neutrally. Second, under certain conditions, the use of phylograms can also absorb changes in
 351 mutation rate (per loci per generation), which in mammals can vary up to 10 fold (Bergeron et al., 2023).
 352 As in the case of our simulations, we assumed that the genetic architecture of the trait is constant and the
 353 mutation rate is homogeneous across the genome. However, if the mutation rate would only change for a
 354 subset of the genome that is encoding the trait, the phylogram would not absorb these changes in mutation
 355 rate. Finally, because chronograms are usually derived from phylograms by calibrating the tree with molecular
 356 clocks, using phylograms directly has the additional advantage of removing model assumptions required to
 357 calibrate node ages (Litsios and Salamin, 2012).

358 These examples show that while phylograms are useful to model neutral evolution, caution is still war-
 359 ranted. In our simulations, we generally found that using a phylogram tends to favour the OU process over
 360 BM. This suggests that trees in units of nucleotide divergence may not always provide a reliable framework
 361 for modelling trait evolution, especially when selection is involved. We recommend continuing to use chrono-
 362 grams for modelling selection acting on a trait, as they generally provide more accurate and reliable results.
 363 Moreover, for a trait under selection for which the pace of optimum changes is also tracking the changes in
 364 generation time, the support for a phylogram over a chronogram would be misleading (Litsios and Salamin,
 365 2012). Therefore, we argue that while phylograms can offer valuable insights (Wilson et al., 2022), they
 366 should be used with caution and in conjunction with chronograms to provide a more comprehensive under-
 367 standing of trait evolution. Contrarily to our cautious note, Wilson et al. (2022) suggested that phylograms
 368 are more robust for studying discrete character evolution than chronogram. This apparent contradiction is
 369 due to the different units of measurement used in the studies, as they measure branch lengths in units of
 370 morphological distance rather than substitutions per site (Wilson et al., 2022). We thus argue that the use
 371 of a phylogram, measured in units of substitutions, could also be useful for studying the evolution of discrete
 372 characters, but the same caution should be applied.

373 Caution is indeed warranted, as there are several limitations to our approach. First, we simulated only a
 374 subset of different regimes of selection. Notably, we did not simulate a static OU process (with a constant
 375 optimum), which would presumably favour an OU model; such simulations are outside the scope of this
 376 study since our focus is on distinguishing neutral evolution from selection tracking a moving optimum. As
 377 emphasized by Grabowski et al. (2023), the main value of OU models lies in multi-optimum variants that
 378 can detect shifts between selective regimes. But more complex scenarios could be included, for example with
 379 primary and secondary moving optima (Hansen, 2024).

380 Additionally, the simulated genetic architecture of a single trait is assumed to be constant across the
 381 phylogeny. A more realistic genetic architecture should include pleiotropy, epistasis and linkage disequilib-
 382 rium, while here we only considered non-linked loci contributing additively to a single trait. Second, while
 383 the tested alternative models of evolution (multi-rates BM, OU, multi-optimum OU) are standard, they do

384 not encompass the full breadth of available methods to model trait evolution (Höhna et al., 2016; Pennell
 385 et al., 2014). Finally, the mammalian dataset (brain and body) may not be representative of all traits or
 386 species and even though our analysis showcases the utility of phylograms, more empirical studies are needed
 387 to replicate the findings.

388 Gene expression levels (both mRNA and protein levels) represent one class of traits where distinguishing
 389 neutral evolution from different regimes of selection is particularly important. While the polygenic nature of
 390 expression traits can vary, testing whether their evolution is better explained by phylograms or chronograms
 391 can help determine whether changes are driven by accumulation of neutral substitutions or by selection
 392 responding to environmental changes. Indeed, the regime of selection acting on gene expression level is the
 393 focus of intense debate (Bertram et al., 2023; Dimayacyac et al., 2023; Price et al., 2022; Signor and Nuzhdin,
 394 2018). Typically, datasets on which BM is favoured over other models is interpreted as mRNA expression
 395 level evolving neutrally (Catalán et al., 2019; Dimayacyac et al., 2023; Khaitovich et al., 2006). Phenotypic
 396 distance is also plotted as a function of time while claiming that a trait is evolving under drift (Jiang et al.,
 397 2023). Instead, we argue that phenotypic distance should be expressed in units of substitutions instead
 398 of time, using the square root of branch lengths. More generally, from an empirical perspective, the use of
 399 nucleotide changes at neutral loci as a normalizing factor brings new perspectives into trait evolution (Latrille
 400 et al., 2024).

401 Altogether, our study supports the use of a chronogram when testing for selection acting on a trait.
 402 We propose the phylogram-chronogram comparison as a new tool in the comparative methods toolbox,
 403 particularly useful when assessing whether a trait is evolving neutrally or under selection tracking a moving
 404 optimum. In such cases, comparing the support for a phylogram versus a chronogram provides an additional
 405 diagnostic to assess the regime of evolution acting on a trait. We provide a Bayesian model implemented in
 406 *RevBayes* to perform this comparison, which estimates whether BM supports a phylogram or a chronogram
 407 ($0 \leq \pi \leq 1$), given the data at the tip of the tree and both trees with the same topology. For empiricists more
 408 familiar with maximum likelihood approaches, we also provide an implementation that yields comparable
 409 results through AIC weights (see supplementary material section S5). Only if the phylogram has more
 410 support than the chronogram (π close to 1) should one consider the neutral model of evolution as a plausible
 411 explanation for the evolution of the trait, but claims of neutral evolution should still be made cautiously.

412 **Supplementary material**

413 Supplementary material is available online at *Evolution Letters*.

414 **Data and code availability**

415 The materials that support the findings of this study are openly available in GitHub at
 416 github.com/ThibaultLatrille/ChronoPhylogram. Snakemake pipeline, simulator, analysis scripts and
 417 *RevBayes* scripts and documentation are available in the repository to replicate the study.

418 **Author contributions**

419 Original idea: T.L.; Model conception: T.L., T.G. and N.S.; Code: T.L.; Data analyses: T.L. and T.G.;
 420 Interpretation: T.L., T.G. and N.S.; First draft: T.L.; Editing and revisions: T.L., T.G. and N.S. Project
 421 management and funding: N.S.

422 **Funding**

423 This work was funded by Faculté de Biologie et de Médecine, Université de Lausanne (<https://www.unil.ch>;
424 to TL, TG and NS) and Swiss National Science Fund (<https://www.snf.ch>; grant 315230-219757 to TL and
425 NS). The funders did not play any role in the study design, data collection and analysis, decision to publish,
426 or preparation of the manuscript.

427 **Conflict of interest**

428 The authors declare no conflicts of interest.

429 **Acknowledgements**

430 We gratefully acknowledge the help of Lucy M. Fitzgerald, Diego A. Hartasánchez, Anna Marcionetti and
431 Julien Joseph for their advice and reviews concerning this manuscript. We also thank an anonymous reviewer
432 of our previous study (neutrality index for a trait) for commenting on the use of phylogram to test for neutral
433 evolution, which sparked the idea of this study. Finally, we thank the editor and two anonymous reviewers
434 for their constructive comments and suggestions.

435 **References**

- 436 Barton, N. H., Etheridge, A. M., and Véber, A. (2017). The infinitesimal model: Definition, derivation, and
437 implications. *Theoretical Population Biology*, 118:50–73.
- 438 Beaulieu, J. M., Jhwueng, D.-C., Boettiger, C., and O’Meara, B. C. (2012). Modeling stabilizing selection:
439 Expanding the Ornstein-Uhlenbeck model of adaptive evolution. *Evolution*, 66(8):2369–2383.
- 440 Bergeron, L. A., Besenbacher, S., Zheng, J., Li, P., Bertelsen, M. F., Quintard, B., Hoffman, J. I., Li, Z.,
441 St. Leger, J., Shao, C., Stiller, J., Gilbert, M. T. P., Schierup, M. H., and Zhang, G. (2023). Evolution of
442 the germline mutation rate across vertebrates. *Nature*, pages 1–7.
- 443 Bertram, J., Fulton, B., Tourigny, J. P., Peña-Garcia, Y., Moyle, L. C., and Hahn, M. W. (2023). CAGEE:
444 Computational Analysis of Gene Expression Evolution. *Molecular Biology and Evolution*, 40(5):msad106.
- 445 Butler, M. A. and King, A. A. (2004). Phylogenetic comparative analysis: A modeling approach for adaptive
446 evolution. *The American naturalist*, 164(6):683–695.
- 447 Catalán, A., Briscoe, A. D., and Höhna, S. (2019). Drift and directional selection are the evolutionary forces
448 driving gene expression divergence in eye and brain tissue of *Heliconius* butterflies. *Genetics*, 213(2):581–
449 594.
- 450 Cooper, N., Thomas, G. H., Venditti, C., Meade, A., and Freckleton, R. P. (2016). A cautionary note on
451 the use of Ornstein Uhlenbeck models in macroevolutionary studies. *Biological Journal of the Linnean
452 Society*, 118(1):64–77.
- 453 De Magalhães, J. P. and Costa, J. (2009). A database of vertebrate longevity records and their relation to
454 other life-history traits. *Journal of Evolutionary Biology*, 22(8):1770–1774.
- 455 Dimayacyac, J. R., Wu, S., Jiang, D., and Pennell, M. (2023). Evaluating the Performance of Widely Used
456 Phylogenetic Models for Gene Expression Evolution. *Genome Biology and Evolution*, page evad211.
- 457 Eastman, J. M., Alfaro, M. E., Joyce, P., Hipp, A. L., and Harmon, L. J. (2011). A Novel Comparative
458 Method for Identifying Shifts in the Rate of Character Evolution on Trees. *Evolution*, 65(12):3578–3589.

- 459 Felsenstein, J. (1985). Phylogenies and the Comparative Method. *The American Naturalist*, 125(1):1–15.
- 460 Felsenstein, J. (1988). Phylogenies and quantitative characters. *Annual Review of Ecology and Systematics*,
461 19(1):445–471.
- 462 Foley, N. M., Mason, V. C., Harris, A. J., Bredemeyer, K. R., Damas, J., Lewin, H. A., Eizirik, E., Gatesy,
463 J., Karlsson, E. K., Lindblad-Toh, K., Zoonomia Consortium, Springer, M. S., and Murphy, W. J. (2023).
464 A genomic timescale for placental mammal evolution. *Science*, 380(6643):eabl8189.
- 465 Genereux, D. P., Serres, A., Armstrong, J., Johnson, J., Marinescu, V. D., Murén, E., Juan, D., Bejerano,
466 G., Casewell, N. R., Chemnick, L. G., Damas, J., Di Palma, F., Diekhans, M., Fiddes, I. T., Garber,
467 M., Gladyshev, V. N., Goodman, L., Haerty, W., Houck, M. L., Hubley, R., Kivioja, T., Koepfli, K.-P.,
468 Kuderna, L. F. K., Lander, E. S., Meadows, J. R. S., Murphy, W. J., Nash, W., Noh, H. J., Nweeia, M.,
469 Pfenning, A. R., Pollard, K. S., Ray, D. A., Shapiro, B., Smit, A. F. A., Springer, M. S., Steiner, C. C.,
470 Swofford, R., Taipale, J., Teeling, E. C., Turner-Maier, J., Alfoldi, J., Birren, B., Ryder, O. A., Lewin,
471 H. A., Paten, B., Marques-Bonet, T., Lindblad-Toh, K., Karlsson, E. K., and Zoonomia Consortium (2020).
472 A comparative genomics multitool for scientific discovery and conservation. *Nature*, 587(7833):240–245.
- 473 Grabowski, M., Pienaar, J., Voje, K. L., Andersson, S., Fuentes-González, J., Kopperud, B. T., Moen, D. S.,
474 Tsuboi, M., Uyeda, J., and Hansen, T. F. (2023). A Cautionary Note on “A Cautionary Note on the Use
475 of Ornstein Uhlenbeck Models in Macroevolutionary Studies”. *Systematic Biology*, 72(4):955–963.
- 476 Hansen, T. F. (1997). Stabilizing selection and the comparative analysis of adaptation. *Evolution*, 51(5):1341–
477 1351.
- 478 Hansen, T. F. (2024). Three modes of evolution?Remarks on rates of evolution and time scaling. *Journal of*
479 *Evolutionary Biology*, page voae071.
- 480 Hansen, T. F. and Martins, E. P. (1996). Translating between microevolutionary process and macroevolu-
481 tionary patterns: The correlation structure of interspecific data. *Evolution*, 50(4):1404–1417.
- 482 Hansen, T. F., Pienaar, J., and Orzack, S. H. (2008). A comparative method for studying adaptation to a
483 randomly evolving environment. *Evolution*, 62(8):1965–1977.
- 484 Harmon, L. (2018). Phylogenetic comparative methods: Learning from trees.
- 485 Höhna, S., Landis, M. J., Heath, T. A., Boussau, B., Lartillot, N., Moore, B. R., Huelsenbeck, J. P., and Ron-
486 quist, F. (2016). RevBayes: Bayesian Phylogenetic Inference Using Graphical Models and an Interactive
487 Model-Specification Language. *Systematic Biology*, 65(4):726–736.
- 488 Holstad, A., Voje, K. L., Opedal, Ø. H., Bolstad, G. H., Bourg, S., Hansen, T. F., and Pélabon, C. (2024).
489 Evolvability predicts macroevolution under fluctuating selection. *Science*, 384(6696):688–693.
- 490 Ingram, T. and Mahler, D. (2013). SURFACE: Detecting convergent evolution from comparative data by
491 fitting Ornstein-Uhlenbeck models with stepwise Akaike Information Criterion. *Methods in Ecology and*
492 *Evolution*, 4(5):416–425.
- 493 Jiang, D., Cope, A. L., Zhang, J., and Pennell, M. (2023). On the Decoupling of Evolutionary Changes in
494 mRNA and Protein Levels. *Molecular Biology and Evolution*, 40(8):msad169.
- 495 Khabbazian, M., Kriebel, R., Rohe, K., and Ané, C. (2016). Fast and accurate detection of evolutionary
496 shifts in Ornstein–Uhlenbeck models. *Methods in Ecology and Evolution*, 7(7):811–824.
- 497 Khaitovich, P., Enard, W., Lachmann, M., and Pääbo, S. (2006). Evolution of primate gene expression.
498 *Nature Reviews Genetics*, 7(9):693–702.
- 499 Kimura, M. (1968). Evolutionary rate at the molecular level. *Nature*, 217(5129):624–626.

- 500 Kimura, M. (1983). *The Neutral Theory of Molecular Evolution*. Cambridge University Press.
- 501 Lande, R. (1976). Natural selection and random genetic drift in phenotypic evolution. *Evolution*, 30(2):314–
502 334.
- 503 Lande, R. (1980). The genetic covariance between characters maintained by pleiotropic mutations. *Genetics*,
504 94(1):203–215.
- 505 Latrille, T., Bastian, M., Gaboriau, T., and Salamin, N. (2024). Detecting diversifying selection for a trait
506 from within and between-species genotypes and phenotypes. *Journal of Evolutionary Biology*, 37(12):1538–
507 1550.
- 508 Litsios, G. and Salamin, N. (2012). Effects of Phylogenetic Signal on Ancestral State Reconstruction. *Sys-*
509 *tematic Biology*, 61(3):533–538.
- 510 Lynch, M. (1990). The Rate of Morphological Evolution in Mammals from the Standpoint of the Neutral
511 Expectation. *The American Naturalist*, 136(6):727–741.
- 512 Lynch, M. and Hill, W. G. (1986). Phenotypic evolution by neutral mutation. *Evolution*, 40(5):915–935.
- 513 Mitov, V., Bartoszek, K., Asimomitis, G., and Stadler, T. (2020). Fast likelihood calculation for multivariate
514 Gaussian phylogenetic models with shifts. *Theoretical Population Biology*, 131:66–78.
- 515 Nielsen, J., Hedeholm, R. B., Heinemeier, J., Bushnell, P. G., Christiansen, J. S., Olsen, J., Ramsey, C. B.,
516 Brill, R. W., Simon, M., Steffensen, K. F., and Steffensen, J. F. (2016). Eye lens radiocarbon reveals
517 centuries of longevity in the Greenland shark (*Somniosus microcephalus*). *Science*, 353(6300):702–704.
- 518 Ohta, T. (1972). Population size and rate of evolution. *Journal of Molecular Evolution*, 1(4):305–314.
- 519 Paradis, E., Claude, J., and Strimmer, K. (2004). APE: Analyses of Phylogenetics and Evolution in R
520 language. *Bioinformatics*, 20(2):289–290.
- 521 Pennell, M. W., Eastman, J. M., Slater, G. J., Brown, J. W., Uyeda, J. C., FitzJohn, R. G., Alfaro, M. E.,
522 and Harmon, L. J. (2014). Geiger v2.0: An expanded suite of methods for fitting macroevolutionary models
523 to phylogenetic trees. *Bioinformatics*, 30(15):2216–2218.
- 524 Price, P. D., Palmer Drogue, D. H., Taylor, J. A., Kim, D. W., Place, E. S., Rogers, T. F., Mank, J. E.,
525 Cooney, C. R., and Wright, A. E. (2022). Detecting signatures of selection on gene expression. *Nature*
526 *Ecology & Evolution*, pages 1–11.
- 527 Sella, G. and Barton, N. H. (2019). Thinking about the evolution of complex traits in the era of genome-wide
528 association studies. *Annual Review of Genomics and Human Genetics*, 20(1):461–493.
- 529 Signor, S. A. and Nuzhdin, S. V. (2018). The Evolution of Gene Expression in cis and trans. *Trends in*
530 *Genetics*, 34(7):532–544.
- 531 Silvestro, D., Kostikova, A., Litsios, G., Pearman, P. B., and Salamin, N. (2015). Measurement errors
532 should always be incorporated in phylogenetic comparative analysis. *Methods in Ecology and Evolution*,
533 6(3):340–346.
- 534 Silvestro, D., Tejedor, M. F., Serrano-Serrano, M. L., Loiseau, O., Rossier, V., Rolland, J., Zizka, A., Höhna,
535 S., Antonelli, A., and Salamin, N. (2019). Early Arrival and Climatically-Linked Geographic Expansion
536 of New World Monkeys from Tiny African Ancestors. *Systematic Biology*, 68(1):78–92.
- 537 Soria, C. D., Pacifici, M., Di Marco, M., Stephen, S. M., and Rondinini, C. (2021). COMBINE: A coalesced
538 mammal database of intrinsic and extrinsic traits. *Ecology*, 102(6):e03344.
- 539 Tsuboi, M., van der Bijl, W., Kopperud, B. T., Erritzøe, J., Voje, K. L., Kotrschal, A., Yopak, K. E., Collin,
540 S. P., Iwaniuk, A. N., and Kolm, N. (2018). Breakdown of brain–body allometry and the encephalization
541 of birds and mammals. *Nature Ecology & Evolution*, 2(9):1492–1500.

- 542 Turelli, M. (1984). Heritable genetic variation via mutation-selection balance: Lerch's zeta meets the ab-
543 dominal bristle. *Theoretical Population Biology*, 25(2):138–193.
- 544 Turelli, M. (1988). Phenotypic Evolution, Constant Covariances, and the Maintenance of Additive Variance.
545 *Evolution*, 42(6):1342–1347.
- 546 Uyeda, J. C. and Harmon, L. J. (2014). A Novel Bayesian Method for Inferring and Interpreting the Dynamics
547 of Adaptive Landscapes from Phylogenetic Comparative Data. *Systematic Biology*, 63(6):902–918.
- 548 Wilson, J. D., Mongiardino Koch, N., and Ramírez, M. J. (2022). Chronogram or phylogram for ancestral
549 state estimation? Model-fit statistics indicate the branch lengths underlying a binary character's evolution.
550 *Methods in Ecology and Evolution*, 13(8):1679–1689.